Optical Society of America. J. S. Sanghera, F. H. Kung, P. C. Pureza, V. Q. Nguyen, R. E. Miklos, and I. D. Aggarwal, "Infrared evanescent-absorption spectroscopy with chalcogenide glass fibers," Appl. Opt. 33, 6315-6322 (1994). doi: 10.1364/AO.33.006315

Infrared evanescent-absorption spectroscopy with chalcogenide glass fibers

J. S. Sanghera, F. H. Kung, P. C. Pureza, V. Q. Nguyen, R. E. Miklos, and I. D. Aggarwal

We have used telluride glass fibers fabricated in house to measure the evanescent-absorption spectra of water, methanol, ethanol, isopropanol, acetone, ethanoic acid, hexane, and chloroform. Furthermore, detection limits of less than 2 vol. % solute were obtained for mixtures of water and methanol, ethanol, isopropanol, acetone, and ethanoic acid. Techniques to reduce the detection limits are discussed.

Key words: Chalcogenide glass fiber, remote IR spectroscopy, evanescent absorption, fiber-optic sensors.

Introduction

To date most of the optical fibers used in remote absorption-type chemical sensors have been based on silica[1,2] and to a lesser extent on fluoride glass fibers.[3] However, these fibers exhibit significant multiphonon absorption beyond 3 and 4 μm, respectively, and are therefore inappropriate materials for use beyond 4 μm.[4] Because most chemical species possess characteristic vibrational signatures between 2 and 12 μm, alternative longer-wavelength transmitting materials are needed. Chalcogenide glasses are ideal candidate materials because they transmit between 2 and 12 μm and therefore encompass the IR region of interest for remote chemical spectroscopy. Chalcogenide glasses are made from mixtures of the chalcogen elements S, Se, and Te, and the addition of other elements such as Ge, As, and Sb facilitates stable glass formation.[5] The use of chalcogenide glass fibers for remote chemical sensing is very promising, not only because of these glasses' optical properties but also because of their chemical durability. Although these glasses cannot be used in strongly basic environments because they undergo chemical attack, there are numerous environments in which they can be used. For example, the glasses do not react with water, unlike fluoride glasses, and can therefore be used in aqueous environments. In addition, the glasses can also be used in acidic and organic environments. Despite these glasses' technological importance,[6] there are only a handful of papers devoted to chalcogenide glass fibers used in remote chemical sensors.[7–10]

In the present paper we demonstrate the application of our own in-house-fabricated telluride glass fibers for recording the absorption spectra of eight liquids: methanol, ethanol, isopropanol, acetone, ethanoic acid, water, hexane, and chloroform. In addition, because the first five chemicals are completely soluble in water, their mixtures with water were also studied, and the respective detection limits are identified. Finally, we make some recommendations to lower the detection limits by optimization of the sensor design.

Experimental

The composition of our glass fibers approached the nominal $Ge_{30}As_{10}Se_{30}Te_{30}$ composition (at. %). The quality of the elemental precursors is, however, not sufficient to fabricate good-quality fibers. Hence the precursors were further purified in house to remove oxide contamination and other extraneous particles.[11] The purified chemicals were batched in 10-g aliquots in quartz ampoules inside a dry box and under a dry nitrogen atmosphere. The ampoules were evacuated to 10^{-5} Torr and then sealed with a methane–oxygen torch. These ampoules were then melted at 900 °C for 8 h in a rocking furnace to facilitate melting. The ampoules were then quenched and annealed from approximately 265 °C. The rods were removed from the ampoules and subsequently drawn

J. S. Sanghera, P. C. Pureza, and I. D. Aggarwal are with the Naval Research Laboratory, Code 5603.2, Washington, D.C. 20375; F. H. Kung is with the University of Maryland Research Foundation, Greenbelt, Maryland 20770; V. Q. Nguyen is with the Department of Electrical Engineering, Virginia Polytechnic Institute, Blacksburg, Virginia 24061; and R. E. Miklos is with SFA Inc., Landover, Maryland 20785.

Received 15 October 1993; revised manuscript received 4 March 1994.

0003-6935/94/276315-08$06.00/0.

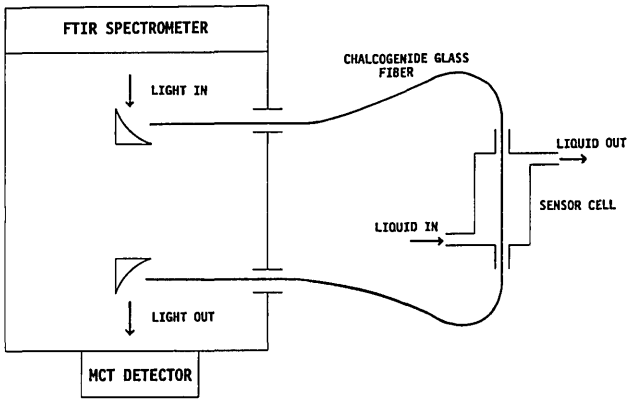

Fig. 1. Schematic representation of the chemical sensor setup. MCT, mercury cadmium telluride.

into fibers in a specially designed narrow-hot-zone furnace under a dry nitrogen atmosphere and inside a class 100 clean room. The fibers were drawn at around 400 °C and at 0.5–2 m/min depending on fiber size. The attenuation of the fiber was measured by the use of the cutback technique with a Fourier transform infrared (FTIR) spectrometer (Bomem DA8), following the technique described by Driver *et al.*[12]

The setup for the sensor experiments is shown in Fig. 1. The light from a broadband glow bar source inside the FTIR was focused onto a 200-μm-diameter, 1.5-m-long fiber with a 0.21-N.A. off-axis parabolic mirror. Approximately 75 cm from the start of the fiber, an 18-cm section of the fiber was enclosed in a Pyrex cell, which was designed so that liquids could be easily poured into and drained out of the system. Thereafter the fiber was directed back into the FTIR, where a similar parabolic mirror was used to direct the light from the fiber onto a liquid-nitrogen-cooled HgCdTe (mercury cadmium telluride) detector. The baseline spectrum of the fiber was recorded before the addition of the liquids into the cell. The liquids were then poured into the cell, and the spectra were recorded and subsequently referenced to the baseline spectrum. In all cases, 100 scans were recorded, which took approximately 42 s, and the resolution used was 4 cm^{-1}.

Two types of sensor experiments were performed. The motivation for the first set of experiments was to see whether we could use our fibers to measure reliable evanescent-absorption spectra. In this case the spectra of eight separate liquids were recorded and compared with the literature data. Table 1 shows a list of the chemicals and their sources. Second, mixtures of water and the liquids methanol, ethanol, isopropanol, acetone, and ethanoic acid were also prepared, and the evanescent-absorption spectra were recorded. The composition of the mixtures is described by the following equation:

$$(x)A.(100 - x)H_2O, \quad (1)$$

where A represents the solute, in this case the other liquid, and x = 0, 2, 20, 50, and 100% volume of solute. These solutes were chosen because they are known to be completely miscible with water.

Table 1. Chemicals and Their Sources

Chemical	Source
Deionized water	MilliPore-Q water system
Methanol	Fisher Scientific (certified ACS[a] grade)
Ethanol	Warner Graham Co. (190 proof)
Isopropanol	Mallinckrodt (analytical reagent grade)
Acetone	Mallinckrodt (analytical reagent grade)
Ethanoic acid	Baker Chemicals (glacial-reagent grade)
Hexane	Fisher Scientific (optima grade)
Chloroform	Fisher Scientific (certified ACS grade)

[a]American Chemical Society.

Results

In Fig. 2, curve (b) shows the measured attenuation spectrum of the 1.5-m length of fiber used in this study. A minimum loss of 0.28 dB/m was obtained at 6.6 μm, and the loss was below 1 dB/m between approximately 5.25 and 9.5 μm. Our fiber attenuation is approximately 5 times lower than the value quoted for the fiber used by Heo *et al.*[10] There is a trace of a band at 7.9 μm whose presence is attributed to the Ge—O combination band.[13] Also shown in Fig. 2 [curve (a)] is the attenuation plot of a fiber coated with an UV-curable acrylate. There are a significant number of absorption bands present that are attributed to the polymer coating.

Figures 3(a)–3(d) show examples of our measured spectra for the pure liquids versus literature data obtained with absorption spectroscopy of the liquids between two salt windows.[14,15] There is excellent agreement between our measured spectra and the literature data. For example, in Fig. 3(a), we show the major bands in water, that is, the fundamental OH stretching vibration at 3 μm and the H—O—H bending vibration at 6.1 μm. For the alcohols, such as isopropranol, shown in Fig. 3(b), the bands at 3 and 3.5 μm are due to the fundamental O—H stretching and the C—H stretching vibrations, respectively.

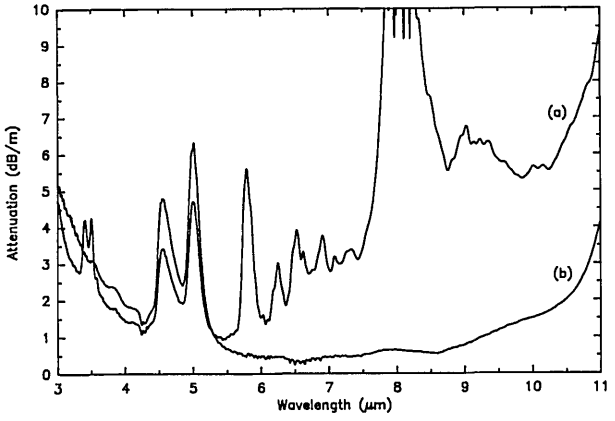

Fig. 2. Attenuation curves for (a) the UV-curable acrylate-coated telluride fiber and (b) the uncoated telluride fiber used in this study.

The bands around 7 μm arise from the CH, CH_2, and CH_3 bending vibrations as well as the OH bending vibration. The bands beyond 8 μm are attributed to the C—O stretching vibration. In acetone, the band at 3.3 μm is due to the C—H stretching vibration, the band at 5.86 μm is due to the C=O stretching vibration, the 7.36-μm band is due to the CH_3 bending vibration, and the ketone functional group vibration [C—C(=O)—C] occurs at 8.2 μm. In glacial ethanoic aid, there are four major absorption bands, which are composed of the C—H and O—H stretching vibrations around 3.3 μm, the C=O stretching vibration at 5.8 μm, the OH bending vibration at 7.1 μm, and the C—O stretching vibration at 7.75 μm. The spectrum for hexane is very simple, consisting of three major bands located at 3.4, 6.8, and 7.25 μm, which are due to the C—H stretching vibration, the CH and CH_2 bending vibrations, and the CH_3 bending vibrational modes, respectively. The spectrum for chloroform contains only one major band located at 8.2 μm, which is attributed to the CH wagging vibration.

Figures 4(a) and 4(b) show the increase in the absorbance of the appropriate vibrational bands with increasing concentration of ethanol and acetone relative to water, respectively. The particular peaks chosen were the most prominent and displayed the least amount of overlap with the peaks from water. In all cases a minimum value of 2 vol. % solute was readily discernible. Also, it is evident that the peak position shifts with increasing concentration of solute. Table 2 lists the peak position and the absorbance versus the concentration of solute for all the mixtures investigated.

Figure 5 shows a representative plot of the peak height (absorbance) versus the concentration of ethanol. All the spectra displayed a linear relationship between absorbance and the concentration of solute.

Figures 6(a) and 6(b) display the variation in the peak position versus concentration of ethanol and acetone in water, respectively. All the solutions exhibit a linear dependence of peak position on solute concentration except for ethanoic acid, where there appears to be some anomalous behavior. This behavior may be related to the significant overlap between the peaks comprising the doublet, therefore making the peak position difficult to ascertain accurately. However, this problem potentially can be solved by deconvolution of the bands. The appropriate peaks all shift to shorter wavelengths with increasing alcohol content, whereas the specific peak in acetone shifts to longer wavelengths with increasing acetone content.

Discussion

We have used evanescent-wave coupling to record the IR absorption spectra of methanol, ethanol, isopropanol, acetone, ethanoic acid, water, hexane, and chloroform between 3 and 11 μm with our in-house-fabricated telluride glass fiber. The results are in excellent agreement with the literature data and highlight the wide transmission window of the telluride fibers. All the chemicals possess major vibrational bands above 6 μm, which are readily accessible by the use of chalcogenide glass fibers but not silica or fluoride glass fibers. Also, the fibers did not exhibit any reaction with these liquids, further emphasizing their inert chemical nature.

Mixtures of water and methanol, ethanol, isopropanol, acetone, and ethanoic acid exhibited a linear relationship between the appropriate peak intensity and the concentration of solute. In all cases the minimum detection limit was 2 vol. % of solute, although no attempt to try a 1 vol. % solute concentration was made. These are the lowest detection limits reported for such mixtures with IR evanescent-absorption spectroscopy, to our knowledge. Our detection limit of 2 vol. % acetone in water was lower than the limit of 5 vol. % reported by Heo *et al.*[10] The difference is attributed to the fact that we analyzed the peak centered at 8.2 μm, which was due to the ketone functional group [C—C(=O)—C], and not the peak at 5.85 μm, which was due to C=O. The problem with the peak at 5.85 μm was that for small concentrations of acetone, this band is obscured by the 6.1-μm absorption band because of the bending vibration of water molecules. Also, our detection limit of 2 vol. % ethanol in water is lower than the 20 vol. % quoted by Zhang *et al.*[9] and the 5 vol. % shown by Heo *et al.*[10] Another reason for our improved detection limits might be related to our slightly longer evanescent path length of 18 cm compared with the literature values of 10 and 15 cm in Refs. 9 and 10, respectively.

The shift in the peak positions versus the solute concentration shown in Fig. 6 is attributed to hydrogen bonding in the mixtures. Similar shifts have been observed by Zhang *et al.*[9] for their ethanol–water mixtures and by Heo *et al.*[10] for their acetone–water and ethanol–water mixtures.

To make recommendations to improve the design of the sensor, one must first look at the theory for evanescent-wave absorption. From attenuated total reflection theory, it is known that the evanescent-wave intensity E is described by an exponential decay function[16]:

$$E = E_0 \exp(-z\gamma), \tag{2}$$

where z is the distance normal to the optical interface and γ is the attenuation coefficient given by

$$\gamma = (2\pi/\lambda_1)(\sin^2\theta - n_{21}^2)^{1/2}, \tag{3}$$

where θ is the angle of incidence; $n_{21} = n_2/n_1$, with n_2 as the medium refractive index and n_1 as the fiber refractive index ($n_2 < n_1$); and λ_1 is the wavelength of light. Total internal reflection occurs between $\pi/2$ and the critical angle θ_c, where

$$\theta_c = \sin^{-1} n_{21}. \tag{4}$$

The parameters that constitute γ are extremely impor-

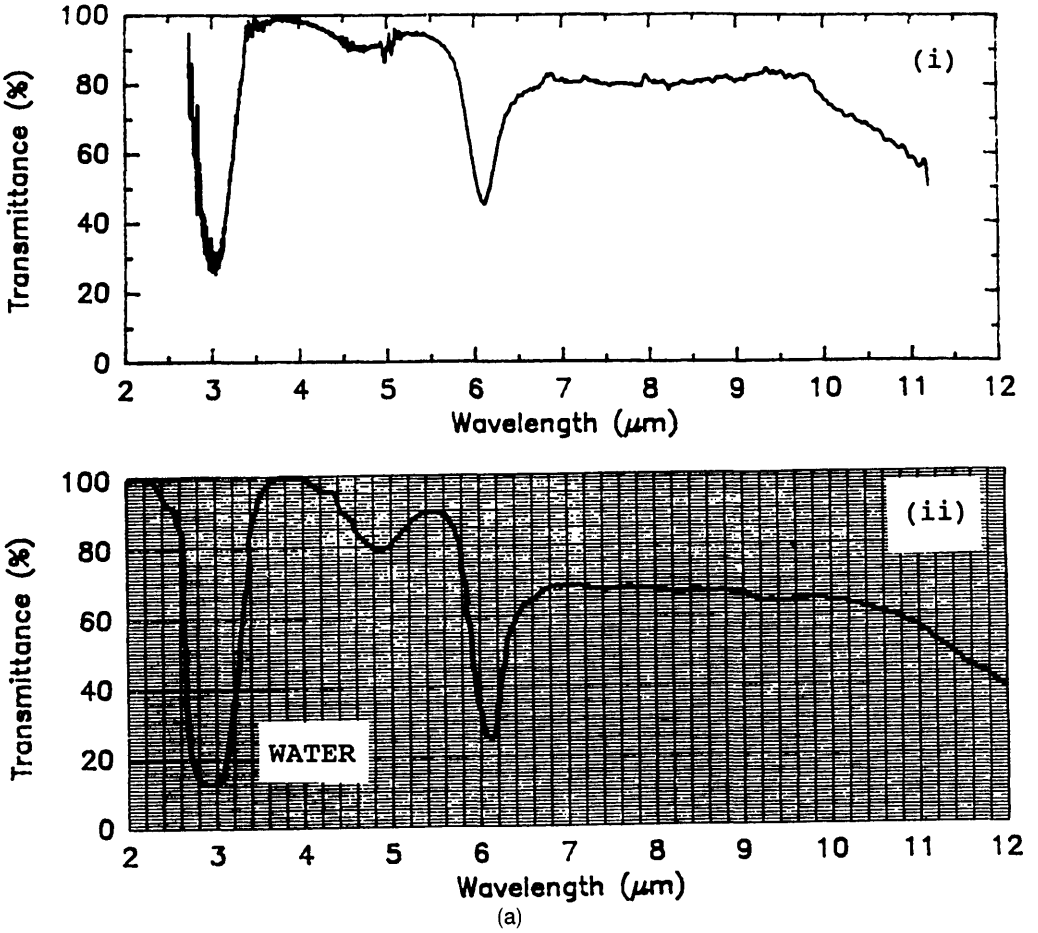

(a)

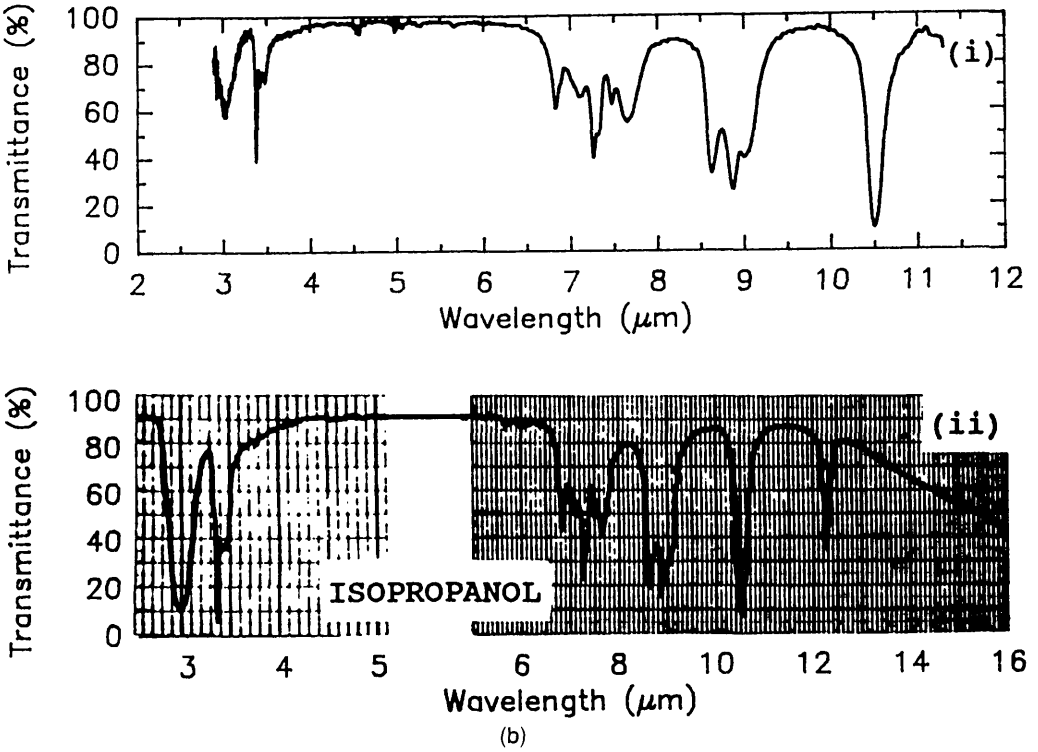

(b)

Fig. 3 continued.

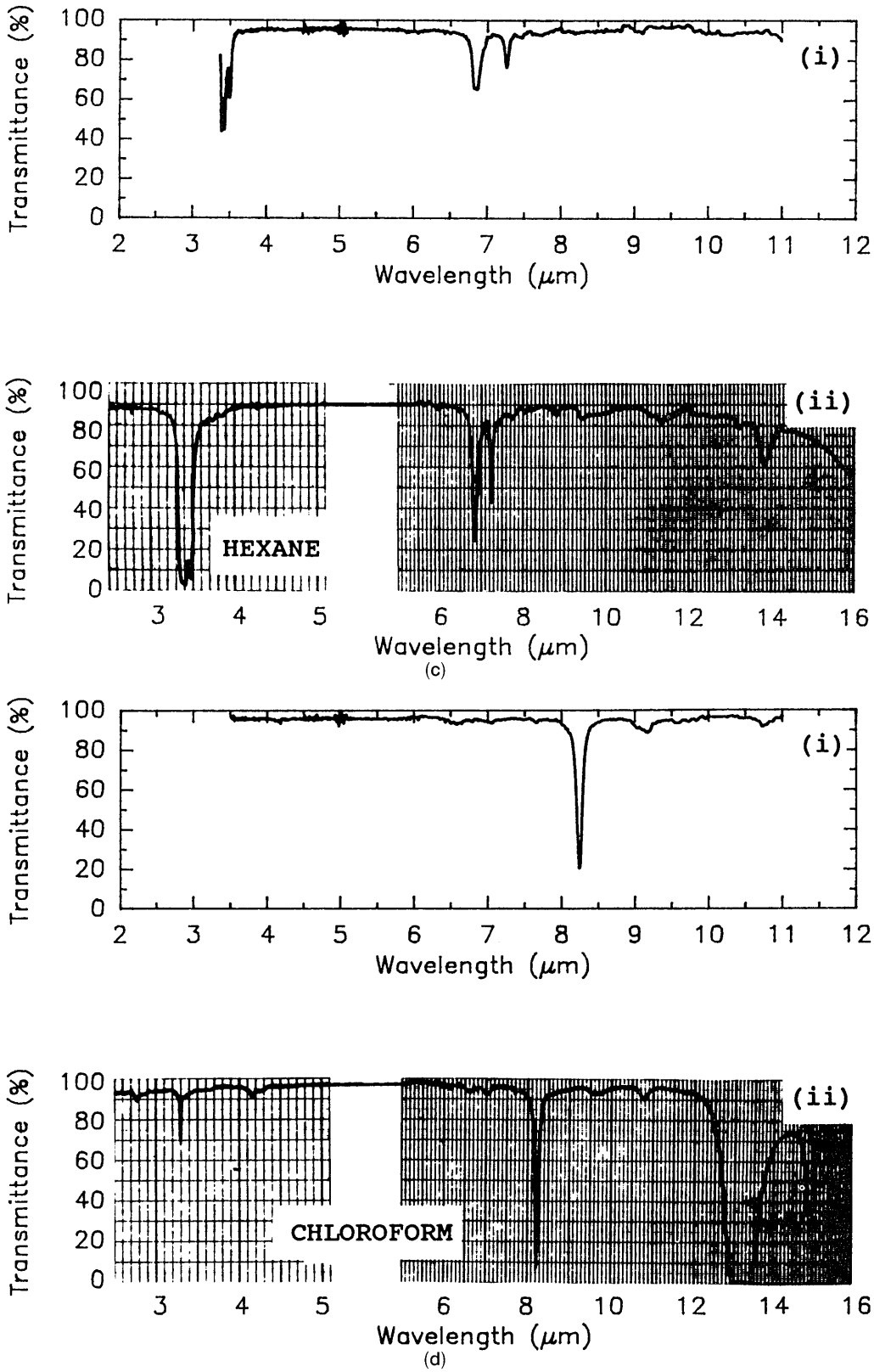

Fig. 3. (i) Measured evanescent-absorption spectra and the (ii) literature absorption data for (a) water, (b) isopropanol, (c) hexane, and (d) chloroform.

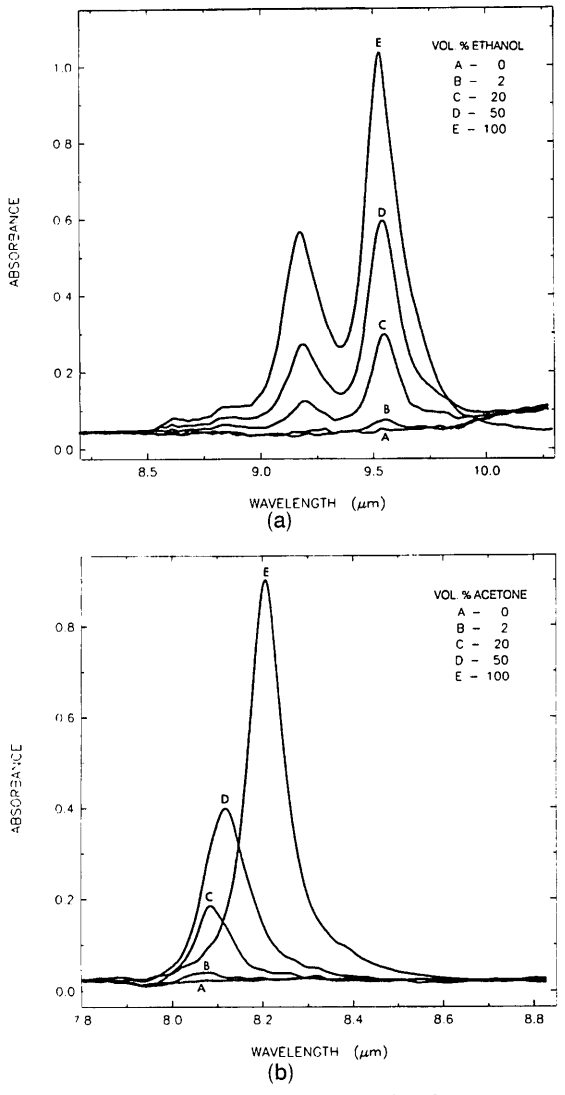

Fig. 4. Spectra displaying the change in absorbance versus the concentration of (a) ethanol and (b) acetone in water.

tant in sensor design, because it is evident from Eq. (2) that lowering γ will increase the intensity of the evanescent wave (E). From Eq. (3), this can be achieved in two ways. First, as the index of the medium approaches that of the fiber, more light becomes available to interact with the medium. Second, γ decreases with wavelength, indicating that the evanescent-wave absorbance becomes more favorable in the IR versus the UV and the visible regions.

Unlike a simple attenuated total reflection experiment, a multimode fiber optic supports many different angles of propagation greater than the critical angle θ_c. Now the θ in Eq. (3) is distributed between $\pi/2$ and θ_c, with the higher-order modes propagating near θ_c. It can be shown that the power distribution is inversely proportional to V, the normalized frequency[16]:

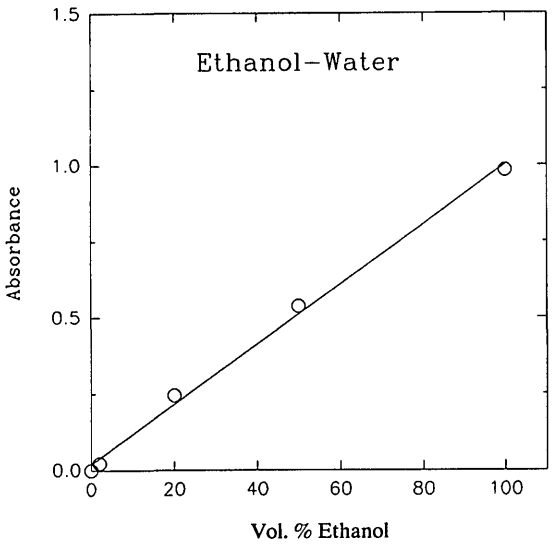

Fig. 5. Plot of the absorbance for the band at 9.5 μm versus the concentration of ethanol in water.

$$V = (2\pi r/\lambda)(n_1^2 - n_2^2)^{1/2}, \quad (5)$$

$$\eta_p = k/V, \quad (6)$$

where r is the fiber radius; λ is the wavelength in free space; η_p is P_m/P_t, where P_m is the evanescent-field intensity in the external medium and P_t is the total light intensity in the core and the external medium; and k is the proportionality constant. One can use a pseudo Beer's law relationship to take into account the power distribution and determine the transmission loss in a fiber evanescent-field sensor of length L as follows:

$$I/I_0 = 10^{-\alpha_e Lc}, \quad (7)$$

where

$$\alpha_e = \eta_p \alpha_c. \quad (8)$$

I is the transmitted intensity in the presence of an absorber, I_0 is the 100% transmission intensity, c is the concentration of solute, and α_c is the Beer's law

Table 2. Peak Position (PP, in micrometers) and Absorbance (Abs) versus Solute Concentration

Solute Concentration (Vol %)	Methanol		Ethanol		Isopropanol		Acetone		Ethanoic Acid	
	PP	Abs	PP	Abs	PP	Abs	PP	Abs	PP	Abs
2	9.853	0.0213	9.573	0.0221	10.596	0.0167	8.056	0.0174	7.795	0.0139
20	9.845	0.2175	9.568	0.2445	10.571	0.1576	8.076	0.1559	7.826	0.2579
50	9.825	0.6617	9.563	0.5371	10.545	0.3964	8.111	0.3752	7.848	0.5480
100	9.754	1.2805	9.533	0.9839	10.494	0.9761	8.188	0.8793	7.742	0.9145

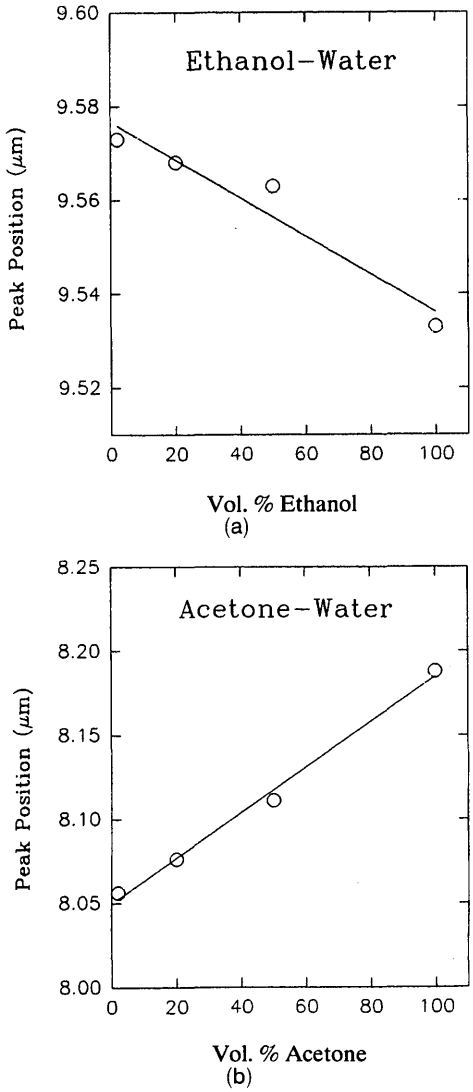

Fig. 6. Relationship between the vibrational-band peak position and the concentration of (a) ethanol and (b) acetone in water.

molar absorptivity of the external medium. Taking the logarithm of Eq. (7) and rearranging it gives us

$$\log_{10}(I_0/I) = \text{absorbance} = \alpha_e L c. \quad (9)$$

This indicates that a linear relationship is expected between the absorbance and the concentration of the solute. In fact the data in Table 2 and the plot in Fig. 5 demonstrate the predicted linear relationship between the absorbance and the concentration of solute. Deviations from linearity are possible because of changes in the N.A. that are caused by the change in the refractive index of the water–solute mixture. However, these changes are considered to be negligible because the indices of the liquids are all around 1.3–1.5, which is much smaller than the index of the glass fiber, which is approximately 2.8. Hence the N.A. is unaffected. In addition, from Eq. (9), the absorbance is also proportional to the fiber sensing length. Therefore the sensitivity of the fiber sensor can be increased by the use of a longer path length. This will subsequently lower the detection limit of the solute. Consequently, the question arises as to what length of sensing fiber would be required for a 100 parts in 10^6 (ppm) detection limit of methanol, for example. If we assume that an 18-cm path-length sensor can detect approximately 1 vol. % methanol, then 18 m of fiber would be required for the sensor to detect 100 ppm of methanol. Because of practical constraints on the length of the sensor, the fiber would obviously be coiled around a small mandrel. In such a case the actual detection limit would be less than 100 ppm because microbending will inevitably redistribute the power from the low-order modes into the higher-order modes, with subsequently greater evanescent penetration. According to Eq. (5), this detection limit would be further enhanced by the use of a smaller fiber radius. Hence the detection limit would be markedly below 100 ppm when one is using 9 m of a 100-μm-diameter fiber coiled on a mandrel. Also, a fiber with a lower refractive index and therefore a smaller N.A. would also result in greater evanescent penetration into the analyte medium. Furthermore, an antireflective coating on the fiber-end faces would serve to increase the amount of light in the fiber and therefore the evanescent penetration. For example, Lucas and Zhang[17] have applied heavy metal fluoride coatings on their chalcogenide glasses and observed an increase from 62% to 96% transmittance in the 8–12-μm region. The addition of reagent-specific coatings to preconcentrate the solute on the fiber surface will also lead to lower detection limits. Finally, we believe that improvements in our fiber quality with the use of optimized processing techniques will lead to lower attenuation in the IR and therefore longer fiber lengths as well as a wider IR transmission window.

Summary

We have used telluride glass fibers fabricated in house to measure the evanescent-absorption spectra of water, methanol, ethanol, isopropanol, acetone, ethanoic acid, hexane, and chloroform. The measured spectra are in excellent agreement with the literature data for these chemicals. Furthermore, mixtures of water and the liquids methanol, ethanol, isopropanol, acetone, and ethanoic acid were also analyzed. As theoretically predicted, we observed a linear relationship between the peak height of the appropriate vibrational bands and the concentration of the solute. The minimum detection limit for these solutes in water was determined to be less than 2 vol. %, and the techniques required for us to lower the detection limits were discussed.

References and Notes

1. H. Tai, H. Tanaka, and T. Yoshino, "Fiber-optic evanescent-wave methane-gas sensor using optical absorption for the 3.392-μm line of a He–Ne laser," Opt. Lett. **12,** 437–439 (1987).
2. F. L. Dickert, S. K. Schreiner, G. R. Mages, and H. Kimmel, "Fiber-optic dipping sensor for organic solvents in wastewater," Anal. Chem. **61,** 2306–2309 (1989).

3. S. J. Saggese, M. R. Shahriari, and G. H. Sigel, Jr., "Fluoride fibers for remote chemical sensing," in *Infrared Optical Materials IV*, S. Musikant, ed., Proc. Soc. Photo-Opt. Instrum. Eng. **929,** 106–114 (1988).
4. J. R. Gannon, "Materials for mid-infrared waveguides," in *Infrared Fibers (0.8–12 μm) I*, L. G. DeShazer and C. Kao, eds., Proc. Soc. Photo-Opt. Instrum. Eng. **266,** 62–68 (1981).
5. Z. U. Borisova, *Glassy Semiconductors* (Plenum, New York, 1981), p. 6.
6. P. Klocek, M. Roth, and R. D. Rock, "Chalcogenide glass optical fibers and image bundles: properties and applications," Opt. Eng. **26,** 88–95 (1987).
7. M. Saito, M. Takizawa, K. Ikegawa, and H. Takami, "Optical remote sensing system for hydrocarbon gases using infrared fibers," J. Appl. Phys. **63,** 269–272 (1988).
8. D. A. C. Compton, S. L. Hill, N. A. Wright, M. A. Druy, J. Piche, W. A. Stevenson, and D. W. Vidrine, "*In situ* FTIR analysis of a composite curing reaction using mid-infrared transmitting optical fiber," Appl. Spectrosc. **42,** 972–979 (1988).
9. X. H. Zhang, M. V. Duhamel, H. L. Ma, C. Blanchetiere, and J. Lucas, "Application of the TeX glass fibers as chemical sensors," J. Non-Cryst. Solids **161,** 327–330 (1993).
10. J. Heo, M. Rodrigues, S. J. Saggese, and G. H. Sigel, Jr., "Remote fiber-optic chemical sensing using evanescent-wave interactions in chalcogenide glass fibers," Appl. Opt. **30,** 3944–3951 (1991).
11. J. S. Sanghera, V. Q. Nguyen, R. Miklos, and I. D. Aggarwal, "Measurement of bulk absorption coefficients of chalcogenide and chalcohalide glasses at 10.6 μm using CO_2 laser calorimetry," J. Non-Cryst. Solids **161,** 320–322 (1993).
12. R. D. Driver, G. M. Leskowitz, L. E. Curtiss, D. E. Moynihan, and L. B. Vacha, "The characterization of infrared transmitting fibers," Mater. Res. Soc. Symp. Proc. **172,** 169–175 (1990).
13. J. A. Savage and S. Nielsen, "Preparation of glasses transmitting in the infrared between 8 and 15 microns," Phys. Chem. Glasses **5,** 82–86 (1964).
14. Provided by Sadtler Research Laboratories, Inc., Philadelphia, Pa.
15. C. J. Pouchert, *The Aldrich Library of FT-IR Spectra* (Aldrich Chemical Company, Milwaukee, Wisc., 1981).
16. M. D. DeGrandpre and L. W. Burgess, "Long path fiber-optic sensor for evanescent field absorbance measurements," Anal. Chem. **60,** 2582–2586 (1988).
17. J. Lucas and X. H. Zhang, "The tellurium halide glasses," J. Non-Cryst. Solids **125,** 1–16 (1990).